Chinese Journal of Polar Science, Vol. 15, No. 2, 91-97, December 2004

Sea ice thickness and concentration in Arctic obtaining from remote sensing images

Lu Peng(卢鹏)[1], Li Zhijun(李志军)[1], Dong Xilu(董西路)[2], Zhang Zhanhai(张占海)[3] and Chen Zhi(陈陟)[4]

1 State Key Laboratory of Coastal and Offshore Engineering, Dalian University of Technology, Dalian 116024, China

2 School of Electronics and Information Engineering, Dalian University of Technology, Dalian 116024, China

3 Polar Research Institute of China, Shanghai 200129, China

4 National Marine Environment Forecasting Center, Beijing 100081, China

Received September 9, 2004

Abstract Based on the sea ice digital videos and photos along the investigation route in the Second Chinese National Arctic Research Expedition (CHINARE) during July and September, 2003, collections of sea ice thickness and concentration in the area of latitude range of 74.11°N-79.56°N and longitude range of 144.17°W-169.95°W are finished. This paper discusses the methods of obtaining ice/snow thicknesses from ship-side videos and ice concentrations from aerial photos, and illustrates the measures should be taken in analysis and in-situ investigation processes to improve the reliability of the parameters. The methods in this paper are somewhat universal and can be used in the research of Bohai Sea and Polar Regions sea ice.

Key words Arctic, sea ice, image, thickness, concentration.

1 Introduction

The Arctic Ocean is one of the important cold regions on the earth, which can affect global climate and ocean circulation seriously. Its interaction with the global climate system is represented by sea ice, which is the main feature on the surface of the Arctic Ocean (Aagaard and Carmack 1989). First, sea ice plays a pivotal role in the heat and mass balance on the surface of the Arctic Ocean. Sea ice not only obstructs the heat exchange between atmosphere and ocean, but also reflects most solar radiation back to the atmosphere because of its high albedo (Greuell *et al.*, 2002). Second, seawater freezing, sea ice melting and movement affect the global water circulation. It is just the movement of sea ice, especially that inside the Arctic Ocean and that transporting outwardly, which provides a direct relation between sea ice and ocean (Lemke *et al.* 1997).

To research the sea ice physical process and the coupled atmosphere-sea ice-ocean model, basic parameters such as ice thickness and concentration are absolutely necessary. The direct method of obtaining these parameters is in situ measurement, but because of the

hostile climate in the polar regions which minimizes human activity, the amount of valid in situ data is limited (Richard *et al*. 2002). As a result satellite observations have been employed to obtain areal coverage of the polar regions. Of particular interest are those satellite observations made in the microwave part of the electromagnetic spectrum due to the ability to obtain data independent of solar luminance and atmosphere conditions. But the complex nature of the interaction of microwaves, and in particular microwaves from active systems, can make data analysis difficult. Moreover because of the extreme height, satellite observation has a low resolution, and can only get ice characteristics in large scale (Gennady and David 2002).

With the development of digital photography, ship-based video and aerial remote sensing are employed to record ice conditions in polar regions expeditions (Stern and Rothrock 1995). Compared with satellite data, these digital images have a higher resolution, and record some ice characteristics in small scale which can not be obtained from satellite data in geophysical scale. Therefore, these digital images can provide supplemental information and help to improve the precision of satellite observation (Garcia *et al*. 2002).

In the First Chinese National Arctic Research Expedition (CHINARE-1999), digital photography had been employed to observe sea ice (Zhao and Ren 2000). In the CHINARE-2003, to improve the precision of satellite observation and compare with in situ measurement, based on the summarization of the 1st Chinese National Arctic Research Expedition and the 19th Chinese National Antarctic Research Expedition, ship-based videos and aerial photos were used for collecting sea ice conditions along the investigation route. These images had a high resolution, were screened continuously, and the responding longitudes and latitudes were recorded synchronously. This paper is to discuss the methods of obtaining ice thickness and ice concentration from the images.

2 Obtaining ice thickness

When a ship sails in the sea area infested by ice, the floating ice can be broken up and reversed under the ship, the cross section of the broken ice may come out of water. If the digital video recorder fixed on the shipboard catches this status, the thickness of the broken ice can be obtained from the image (Worby *et al*. 1996). In CHINARE-2003, to collect ice thickness distribution along the investigation route, a digital video recorder SONY 18E was fixed on the shipboard of *R/V Xuelong* to catch the cross section of broken ice (Fig. 1), the collected signals were transmitted by 1394 data line and stored in a computer. The recording area covered the latitude range of 74.11°N-78.14°N and the longitude range of 169.17°W-149.33°W, all videos lasted 3052s.

To get the absolute value of ice thickness, a red ball of known diameter was hung near the waterline of the ship as a reference, the scene of the video included the cross section of the broken ice and the reference ball (Fig. 2). The method is as follows. First, mark the thickness of the ice cross section and the diameter of the reference ball on the image, as is shown in Fig. 2, where AB is the ice thickness, BC is the thickness of the snow on the ice, and DE is the diameter of the reference ball. Second, record the coordinates of end points of the lines marked above, i.e. point A, B, C, D and E in Fig. 2. At this time the coordinates obtained from images are relative, the unit of which is a pixel. Third, calculate the

distances of AB, BC and DE on the image using the distance formula of two points. Lastly, the actual diameter of the ball is defined as d, according to the similarity criterion, the actual thickness of the ice is $AB \cdot d/DE$; likewise, the actual thickness of the snow on the ice is $BC \cdot d/DE$.

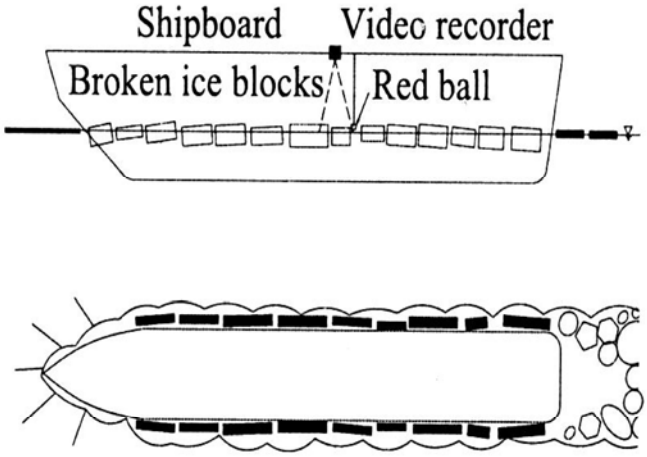

Fig 1 Digital video fixed on shipboard

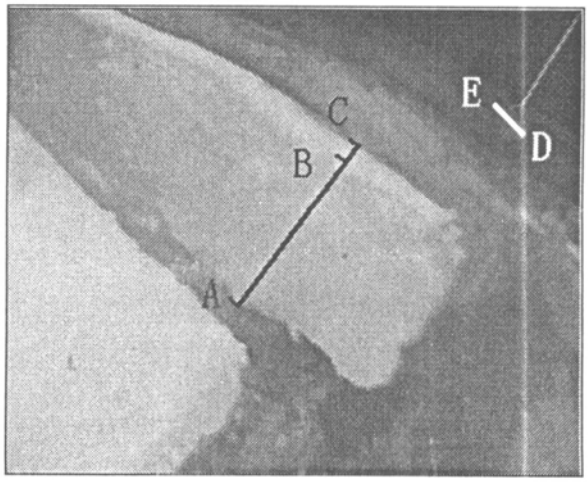

Fig 2 Image from shipboard video

To improve the reliability of this method, some measures had been taken. First, in in situ technique, the reference ball was placed near the waterline and closed to the cross section of broken ice, which can reduce the difference of the distance from the video recorder to the reference ball and to the cross section. Second, in equipment selection, the angle of view of the video recorder was small, which can reduce the effect of image morphing. Lastly, in image process, the digital video with an acquisition frequency of 16Hz was analyzed frame by frame, the same cross section of broken ice may be shot many times. Therefore, thicknesses of the same cross section in different space can be measured from these different images respectively, and then the average value of these thicknesses can be treated as the actual thickness of this ice floe, which can reduce the effect of accidented ice surface and cross section.

Obtaining ice thickness from shipside video is superior to traditional observation by sight, which avoid the bias of a person's estimate. Therefore, this method can provide reliable data and the result can be treated as direct information of ice thickness along the investigation route.

3 Obtaining ice concentration

In CHINARE-2003, a digital camera Canon G2 was fixed on the helicopter *Zhijun*, the sea ice condition below the helicopter was recorded while the helicopter was flying. The digital photos totaled to 4619, covered the latitude range of 75.02°N-79.56°N and the longitude range of 144.17°W-169.59°W, which had a high pixel resolution of 2272 × 1704 and the time interval was 10 seconds, as a sample of which is shown in Fig 3.

The aerial photos contain the information of ice types, states of water leads, characteristics of broken ice around larger floes, distribution of ice ridges and melt ponds on sea ice, etc. But ice concentration is the most important parameter in remote sensing and numeric simulation (Thorsten *et al* 2003), so we get ice concentration from these aerial photos first.

Ice concentration is defined as the proportion of ice covering area in an observation region, usually expressed in tenths, and entered as an integer between 0 and 10. In regions of very high ice concentration (95-99%) where only very small cracks are present, the recorded value should be 10 and the open water classification should be 1 (small cracks). Regions of complete ice cover (100%) will be distinguished by recording an open water classification of 0 (no openings) (Worby 1999). Therefore, if the areas of water and ice have been distinguished from photos respectively, the ice concentration can be work out. Moreover, the purpose of image processing by computer is to confirm the boundary between water and ice, i.e. the threshold value for image segmentation.

For a photo with obvious contrast, the peak value of ice and water can be seen clearly on its gray-level histogram (Fig. 4); here the minimum value on gray-level histogram can be treated as the threshold value (Chen *et al*. 2003). Unfortunately, this method has a big limitation under some conditions. First, when the areas of ice and water are greatly different, there is only one peak value on the histogram. Second, when there is densely foggy, little contrast can be shown in the photo. Then the histogram is very flat, and has no obvious peak or valley. Lastly, sometimes there is more than one minimum value on the gray-level histogram; here it's hard to decide which one should be selected. Under these conditions, this method is not suitable for image segmentation.

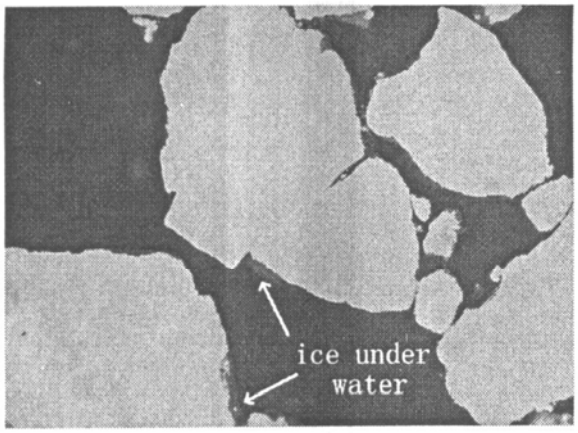

Fig. 3 Aerial image

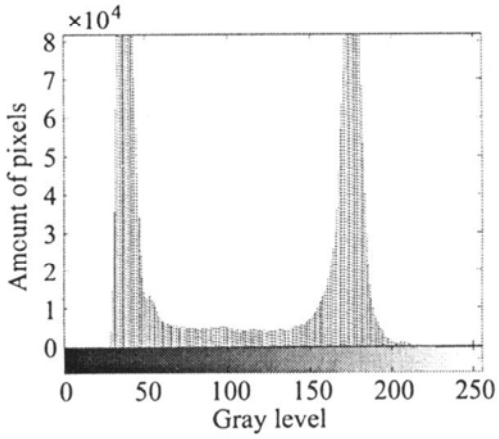

Fig. 4 Gray-level histogram.

After some compares, the *Ostu* method is ensured to be the algorithm of threshold selection in image processing. This method selects the threshold value based on the difference of the image, which considers that a good segmentation method should maximize the difference between the object and the background, that is to say, there will be the highest contrast between the object and the background after segmentation, so this method is also named as the maximum class variance method (Wu *et al*. 2002).

In processing, the method assumes that a threshold value of t can divide the photo X with L gray levels into two classes $C_0 \in [0, t]$, $C_1 \in [t+1, L-1]$, after unifying the histogram, the proportions of pixels at different gray level is given as

$$p_i = \frac{n_i}{N} \qquad p_i \geqslant 0 \qquad \sum_{i=0}^{L-1} p_i = 1 \tag{1}$$

where, N is the total amount of pixels in the photo X, n_i is the amount of pixel at i gray level. Then the probability and the average of C_0 and C_1 can be respectively written as

$$w_0 = p_r(C_0) = \sum_{i=0}^{t} p_i = w(t) \qquad w_1 = p_r(C_1) = \sum_{i=t+1}^{L-1} p_i = 1 - w(t) \tag{2}$$

$$u_0 = \sum_{i=0}^{t} \frac{ip_i}{w_0} = \frac{u(t)}{w(t)} \qquad u_1 = \sum_{i=t+1}^{L-1} \frac{ip_i}{w_1} = \frac{u_T - u(t)}{1 - w(t)} \tag{3}$$

where, $u_T = \sum_{i=0}^{L-1} ip_i$ is the average value of photo X.

The variance of these two classes is

$$\sigma_B^2 = w_0(u_0 - u_T)^2 + w_1(u_1 + u_T)^2 = w_0 w_1 (u_1 - u_0)^2 \tag{4}$$

The optimal threshold value t^* should maximize the variance σ_B^2, then

$$t^* = \arg \max_{0 \leqslant t \leqslant L-1} \sigma_B^2 \tag{5}$$

The *Otsu* method confirms the threshold value based on the thought of maximizing the difference between the object and the background. It has been proved that the *Otsu* method has a high precision through many tests, and most aerial photos get satisfying segmentation results by means of this method. Moreover, the little calculation amount of this method is suitable for batch processing by computer.

The steps of obtaining ice concentration from photos are as follows. First, confirm the threshold value for image segmentation. Second, divide the photo into a binary one by this threshold value, the black and white parts correspond to water and ice respectively. Lastly, calculate the amount of black and white pixels on the binary photo, the proportion of the white pixels is also worked out, that is the ice concentration. A binary photo after segmentation is shown in Fig. 5.

Fig. 5 Binary photo

In analysis of nearly 5000 photos, it was found that the *Otsu* method was suitable for most aerial photos, but for the photos full of ice or water, big errors occurred because of little contrast. So it is necessary to check the results, for the conditions above, ice concentration can be directly set as 0 or 10. In addition, for few photos affected by sunlight or fog, this method can estimate the bright part or fog into ice, it is obviously wrong. Fortunately, there are 124 photos like that in this investigation, only 2.6% of all, they can be processed individually.

On the other hand, there are some floes in the Arctic Ocean, because of disorganization of melt ponds, the cross section of them are not vertical. And then in the photos which is expressed as ice underwater around the floes (Fig. 3). According to the definition of ice concentration, only ice area upon water can be numbered as ice, therefore ice underwater

is numbered as water in image processing. Moreover, the area of ice under water is much smaller the area of ice upon water, so to the ice concentration classified by 10%, this area will not produce any effect.

Obtaining ice concentration from aerial photos by computer processing is superior to traditional observation by sight. First, it is objective, and can not be affected by the bias of a person's estimate. In fact it was just the factitious error in the past that caused the ice concentration needed be classified by 10%. Second, computer processing can increase the resolution of ice concentration to 1%, which is necessary to the improvement of the precision in sea ice numerical simulation. Lastly, in practice computer is used and only individual photos need manual operation, that speed up the image processing as a whole.

4 Summaries

In CHINARE-2003, depending on the video recorder fixed on the shipboard, the ice condition along the investigation route was collected automatically. After analyzing these images frame by frame using the similarity criterion discussing above, the ice/snow thickness distribution along the route was obtained.

Aerial photos were obtained by a camera fixed on the helicopter. The classical *Ostu* method in image segmentation was employed to process these photos, which confirmed the boundary based on the thought of maximizing the difference between the object and the background, and then the ice concentration was obtained.

These methods can avoid the bias of a person's estimate, and the sea ice characteristic parameters obtained from those image data will also provide basic parameters for the analysis of ice distribution along investigation route and help for the further research of coupled atmosphere-sea ice-ocean model, which can be compared with satellite remote sensing data.

Acknowledgements This research was supported by the National Natural Science Foundation of China (40233032) and China Social Commonweal Project (2003DEB5J057). The authors would like to thank Mr. Zhanhai Zhang, Mr. Zhi Chen, Mr. Shan Mei for their collections and contributions the videos and photos. Thanks also to the crew of R/V *Xuelong* and the helicopter *Zhijiu*.

References

Aagaard K, Carmack EC (1989): The role of sea ice and other freshwater in the Arctic circulation. Journal of Geophysical Research, 94(14): 485–14, 498.

Chen DL, Liu JN, Yu LL (2003): Comparison of image segmentation thresholding method. Machine Building & Automation, 1: 77–80 (in Chinese).

Garcia E, Maksym T, Simard M, Dierking W, Van WM, Nghiem SV, Germain K St (2002): A comparison of sea ice field observations in the Barents Sea marginal ice zone with satellite SAR data. Geoscience and Remote Sensing Symposium, IGARSS 02. 2002 IEEE International, 3035–3037.

Gennady IB, David CD (2002): Seasonal comparisons of sea ice concentration estimates derived from SSM/I, OKEAN, and RADARSAT data. Remote Sensing of Environment, 81: 67–81.

Greuell W, Reijmer CH, Oerlemans J (2002): Narrowband-to-broadband albedo conversion for glacier ice and snow based on aircraft and near-surface measurements. Remote Sensing of Environment, 82: 48–63.

Lemke P, Hibler W, Flato G, Harder M, Kreyscher M (1997): On the improvement of sea-ice models for climate simulations: the sea ice model intercomparsion project. Annals of Glaciology, 25: 183-187.

Richard JH, Nick H, Peter W (2002). A systematic method of obtaining ice concentration measurements from ship-based observations. Cold Regions Science and Technology, 34: 97-102.

Stern HL, Rothrock DA (1995). Open water production in Arctic sea ice: Satellite measurements and model parameterizations. Journal of Geophysical Research, 100(20): 601-612.

Thorsten M, Donald JC, Mark AT, Alvaro I (2003): Comparison of aerial video and Landsat 7 data over ponded sea ice. Remote Sensing of Environment, 86: 458-469.

Worby AP (1999): Observing Antarctic sea ice: a practical guide for conducting sea ice observations from vessels operating in the Antarctic pack ice. A CD-ROM produced for the Antarctic Sea Ice Processes and Climate (ASPeCt) Program of the Scientific Committee for Antarctic Research (SCAR) Global Change and the Antarctic (GLOCHANT) Program, Hobart, Australia.

Worby AP, Jeffries MO, Weeks WF, Morris K, Jaña R (1996): The thickness distribution of sea ice and snow cover during late winter in the Bellingshausen and Amundsen Seas, Antarctica. Journal of Geophysical Research, 101(28): 441-455.

Wu W, Liu J, Li X (2002): Research on threshold selection for image segmentation. Journal of XIAN Institute of Technology, 22(4): 309-313(in Chinese).

Zhao JP, Ren JP (2000): Study on the method to analyze parameters of Arctic sea ice from airborne digital imagery. Journal of Remote Sensing, 4(4): 271-278(in Chinese).